

Journal of Materials Chemistry B

Accepted Manuscript



This is an *Accepted Manuscript*, which has been through the Royal Society of Chemistry peer review process and has been accepted for publication.

Accepted Manuscripts are published online shortly after acceptance, before technical editing, formatting and proof reading. Using this free service, authors can make their results available to the community, in citable form, before we publish the edited article. We will replace this *Accepted Manuscript* with the edited and formatted *Advance Article* as soon as it is available.

You can find more information about *Accepted Manuscripts* in the [Information for Authors](#).

Please note that technical editing may introduce minor changes to the text and/or graphics, which may alter content. The journal's standard [Terms & Conditions](#) and the [Ethical guidelines](#) still apply. In no event shall the Royal Society of Chemistry be held responsible for any errors or omissions in this *Accepted Manuscript* or any consequences arising from the use of any information it contains.

Cite this: DOI: 10.1039/c0xx00000x

www.rsc.org/xxxxxx

ARTICLE TYPE

Designed Peptides for Biomineral Polymorph Recognition: A Case Study for Calcium Carbonate

Cite this: DOI: 10.1039/x0xx00000x

Timo Schüler,^a Jochen Renkel,^a Stephan Hobe,^b Moritz Susewind,^a Dorrit E. Jacob,^c Martin Panthöfer,^a Anja Hoffmann-Röder,^a Harald Paulsen,^b Wolfgang Tremel^{a*}

Received 00th January 2014,
Accepted 00th January 2014

DOI: 10.1039/x0xx00000x

www.rsc.org/

With their unique ability for substrate recognition and their sequence-specific self-assembly properties, peptides play an important role in controlling the mineralization of inorganic materials in natural systems and in controlling the assembly of soft materials into complex structures required for biological functions. Here we report the use of an engineered heptapeptide that can differentiate between the crystalline anhydrous polymorphs of calcium carbonate. This peptide contains the positively charged amino acid arginine as well as proline rather than the prototypical negatively charged aspartate or glutamate units. Its affinity to vaterite compared to aragonite was demonstrated by fluorescence microscopy using biotinylated peptides. Crystallization experiments in the presence of vaterite-affine peptide afforded only vaterite, whereas a mutant peptide, where a proline residue was replaced by glycine, exclusively lead to the formation of calcite.

Introduction

Many organisms exhibit highly specific control over mineral formation to generate skeletons and functional biomineral structures based on complex inorganic/organic hybrid materials.¹⁻⁴ Biominerals such as bones, teeth, and mollusk shells serve as an inspiration for engineers to develop new routes towards materials of technological interest.⁵⁻⁸ The formation of these biominerals is under biological control. Ion concentration, compartmentalization, and the concerted action of various biomolecules regulate not only structural features such as polymorph selection, crystal morphology and crystal orientation, but also the reaction pathway through the formation of labile/amorphous intermediates.⁹

The mollusk shell, a heterogeneous composite of two calcium carbonate polymorphs (i.e. calcite and aragonite), is a textbook example of biomineralized hard tissue with a species- and tissue specific distribution of the CaCO₃ polymorphs and an organic matrix.¹⁰ The mechanism underlying the selection of these crystal polymorphs is controversial, but it is accepted to depend on the organic matrix.¹¹⁻¹⁴ The flexible polyelectrolyte hypotheses¹⁵ assumes that the interaction of the organic matrix with the mineral surface depends on charge rather than conformation. An alternative model relies mainly on the stereochemical match between the surface and surface ligands.^{16,17}

One key question for an understanding of biomineralization processes is how the concerted action of proteins and other biomacromolecules can regulate nucleation, crystal growth and self-organization *in vivo*. As the formation of mineral phases occurs in the presence of complex mixtures of macromolecules and ions, attempts have been

made to purify and characterize individual active proteins to understand the mechanism of biomineralization of CaCO₃.¹¹⁻¹⁴ *In vitro* experiments have demonstrated that some proteins found in association with CaCO₃ biominerals, as well as shorter-chain peptides with sequences similar to those found in these proteins, can promote or inhibit nucleation and growth of CaCO₃ aside of any biological context.¹⁸

Vaterite, a metastable anhydrous crystalline polymorph of CaCO₃ occurring in calcified tissues, is particularly intriguing. The crystallization of CaCO₃ progresses, both, *in vitro* and *in vivo*, sequentially according to Ostwald's step rule from amorphous CaCO₃ (ACC) via vaterite and aragonite to calcite, the most stable polymorph; metastable polymorphs like vaterite and aragonite may be skipped under certain circumstances. Although vaterite acts as a precursor for the formation of aragonite or calcite it rarely occurs in nature. It is inherently labile and relatively soluble; still, it has been reported to form and persist in some biological systems, such as gallstones,¹⁹ gastropod eggshells,²⁰ freshwater lacklustre pearls,^{21,22} in a member of the ascidians,²³ the snail, *Biomphalaria glabrata*,²⁴ carp otoliths,²⁵ or sea squirts.²⁶ Here the formation of vaterite is under strict genetic control. Vaterite acts as a transient precursor or functioning for structural purposes. Valiyaveetil and coworker²⁷ isolated pelovaterin, a glycine-rich peptide with 42 amino acid residues and three disulfide bonds, from the eggshells of a soft-shelled turtle. Pelovaterin appears to play a key role in the biomineralization of the turtle eggshell. *In vitro* CaCO₃ crystallization tests showed that pelovaterin induces the formation of vaterite, alters the crystal morphology, and increases its growth rate.²⁷

Recently, it has been demonstrated that short peptides recognize and specifically bind to surfaces of inorganic and organic crystals.²⁸⁻³⁰ These interactions are actuated through Coulomb forces, hydrogen-bonding and van-der-Waals interactions, when the surfaces have a two- or three-dimensional regular distribution of atoms or functional groups. The peptides were selected from libraries displayed on surfaces of genetically engineered cells or phages. Relationships between the individual materials and the selected peptide sequences have been noticed and applications of these material-binding peptides have also been exemplified.²⁸⁻³⁰

At the same time it could be shown that positively charged polymers have an effect on calcium carbonate deposition, leading to the formation of thin films and fibers.³¹ In addition, two novel proteins, Pif (an acidic protein) and Pfn23 (a basic protein), were reported to play a key role in the control over crystal growth in nacre,^{32,33} and *in vitro* crystallization assays revealed them to enhance calcium carbonate deposition. Positively charged basic residues are unexpected components in CaCO₃ binding polymers or proteins. Their presence gives a valuable complementary view to the classic dogma that acidic proteins or common polyelectrolytes such as poly(aspartic acid) exclusively control the deposition of calcium carbonate.⁹⁻¹²

The analysis of the effects of various organic additives (small molecules, amino acids, polymers, etc.) in *in vitro* crystallization assays has produced a virtually unmanageable amount of literature.³⁴ Therefore, exploiting the recognition properties of peptides specific to CaCO₃ would be highly useful. An early phage display study³⁵ using geological calcite yielded a phage, which produced spherical vaterite crystals, but these crystals slowly transformed to calcite under the conditions of precipitation. A second study using commercially available calcite yielded decapeptide glycine amides that retarded the crystallization of calcite from supersaturated solutions.³⁶ Except for a recent mechanistic study by Cölfen *et al.*³⁷ using peptides whose sequences were derived from phage-display assays with aragonite binding affinity we did not encounter any identified sequences in the literature. There is no phage display study using the least stable vaterite polymorph as a template, which is certainly due to the fact that phase pure vaterite was not available until recently.³⁸

Therefore we examined if peptide domains displayed on the surface of the filamentous M13 phage could be used to screen for different polymorphs of calcium carbonate and specifically for vaterite. In phage display screenings using the pIII capsid of the filamentous M13 phage a high frequency of charged acidic amino acids lead to a diminished viability and/or reproduction of phages and therefore to a strongly negative selection. Thus new slightly basic or non-charged, calcium carbonate specific peptides could be identified using the phage display technique. Here we report a phage display selection to identify peptide sequences with affinity and specificity for vaterite. The peptide motifs were selected from commercially available phage libraries displaying heptamer random peptides. By using only short displayed peptide sequences the flexibility of the binding domain is reduced and fewer peptide-surface interactions are allowed, which increases the affinity to vaterite between subsequent generations of selection. With this library, we selected about 60 sequences based on binding affinity. Two of them were synthesized for further investigation: one that exhibited the highest binding affinity (the sequence selected from the third biopanning round) and one with a lower binding affinity to vaterite (selected from the first biopanning round as control). The affinity to vaterite was demonstrated for microcrystal-

line samples by fluorescence microscopy after conjugation to a biotin-streptavidin fluorophore. By applying the same method on a shell of the freshwater bivalve *Diplodon chilensis patagonicus*²¹ we could show the affinity for vaterite being highly selective in the presence of aragonite. Nanoparticle transformation and calcium carbonate precipitation experiments in the presence of the basic vaterite-affine peptide afforded only vaterite with typical "flower-like" morphology, whereas a mutant peptide, whose proline residue was replaced by glycine, lead exclusively to the formation of calcite rhombohedra.

Experimental section

Synthesis of vaterite nanoparticles. The preparation of vaterite nanoparticles was described previously.³⁸ Briefly, 2.5 mmol of calcium chloride dihydrate were dissolved in 25 mL of ethylene glycol and 5 mmol of sodium bicarbonate, dispersed in 25 mL of ethylene glycol, were added. The resulting dispersion was heated up to 40°C and sonicated for 30 minutes. CaCO₃ nanoparticles were separated by centrifugation, washed several times with water and ethanol and dried *in vacuo*.

Phage Display Screening. As prepared nanoparticles were dispersed in TBST-buffer (1 mg mL⁻¹) and 90 μL of this dispersion were mixed with a 10 μL aliquot of the phage library (2.0 × 10⁹ virions) in a LoBind-Eppendorf™ tube. The resulting dispersion was mixed for 1 h on a shaker and centrifuged afterwards. The precipitate was washed six times with TBST and the supernatant was discarded for each time to remove any non-specific binding phages. The bound phages were eluted from the nanoparticles in different ways. In the first and the second panning round the phage-bounded particles were dissolved in 0.2 mol L⁻¹ of pH 2.2 glycine buffer and the solution neutralized afterwards with 1 mol L⁻¹ of Tris base pH 9.1. The phage-bounded particles were incubated in 1 mol L⁻¹ of sodium acetate buffer (pH 8.5) for 30 minutes and centrifuged afterwards. The eluted phages were amplified in 20 mL of a 1:100 dilution of an overnight culture of *Escherichia coli* (ER 2738) grown in sterile LB media at 37°C for 4.5 h. Bacteria were precipitated by centrifugation at 4°C and the supernatants were retained. Phages were precipitated at 4°C overnight by addition of 1/6th the volume of 20% PEG/2.5 mol L⁻¹ sodium chloride. Pelleted phages were separated by centrifugation at 4°C and were re-suspended in 200 μL TBS-buffer.

DNA Purification. After each round of selection, bacteria were infected with dilutions of the eluted phages and subsequently grown upon IPTG/Xgal agar plates. Individual blue colony plaques (minimum 10 plaques) were selected and amplified in 1 mL of a 1:100 dilution of a overnight culture of *E. coli* for 4.5 h at 37°C. The amplified phages were separated as described above, and the single-stranded phage-DNA was collected and purified by addition of 50 μL of TE-saturated phenol and ethanol precipitation afterwards. The DNA was re-suspended in 30 μL sterile distilled water and quantified by gel electrophoresis and UV-Vis spectra at 260 nm. DNA sequencing was done by StarSeq and the sequences were translated into the corresponding peptides using the serial cloner software provided by SerialBasics.

Peptide Synthesis and Analysis. Peptides were synthesized by standard automated Fmoc solid phase peptide synthesis on Rink-amide resins using an ABI 433a peptide synthesizer. Solvents for the peptide syntheses (peptide grade) and coupling-reagents were pur-

chased from Iris Biotech GmbH (Marktredwitz, Germany). Protected Fmoc-L-Amino acids were purchased from Orpegen Peptide Chemicals GmbH (Heidelberg, Germany), except for Fmoc-L-Cys-(Trt)-OH, which was obtained from Novabiochem® Merck KGaA (Darmstadt, Germany). For the peptide syntheses preloaded Tentagel-S-RAM resins with a Rink-amide linker (Rapp Polymere, Tübingen, Germany) were applied.^{39,40} Other chemical reagents were commercially available at the highest possible purity. Optical rotations were measured on a Perkin-Elmer 241 MC Polarimeter at 546 nm and 578 nm, of those the optical rotations at 589,5 nm (sodium-d-line) were then extrapolated. ESI- and HR-ESI-mass spectra were recorded on a Q-TOF Ultima 3 mass spectrometer (micromass/Waters, Milford, Massachusetts-USA). RP-HPLC analyses were carried out on a JASCO-HPLC system (PU-2080Plus pump, DG-2080-53 degaser, LG-2080-02 ternary mixer, MD-2010Plus diode array detector) with Phenomenex Jupiter C18(2) (250 × 4.6 mm, 5 μm) column at a flow rate of 1 mL/min. Preparative HPLC runs were performed on a JASCO-HPLC system (two PU-2087Plus pumps, UV-2075Plus detector) with Phenomenex Jupiter C18(2) (250 × 30 mm, 10 μm) column at a flow rate of 20 mL/min. 2D-NMR spectra were recorded on a Bruker AM 400 or a Bruker DRX 600 spectrometer. Chemical shifts are reported in ppm relative to residual DMSO (¹H spectra: δ = 2.5 ppm; ¹³C spectra: δ = 39.5 ppm). Multiplicities are given as: s (singlet), bs (broad singlet), d (doublet), t (triplet), dd (doublet of doublet), ddd (doublet of doublet of doublet), q (quartet), dq (doublet of quartet), pd (pseudo-doublet), pt (pseudo-triplet), pq (pseudo-quartet), pdd (pseudo-doublet of doublet) and m (multiplet). The peptide syntheses were performed in an Applied Biosystems (life technology, Carlsbad, California, USA) peptide synthesizer ABI 433a combined with an external Perkin-Elmer Series 200 UV/vis-detector.

General procedure for the automated solid-phase peptide syntheses. For the peptide syntheses 0.1 mmol of the corresponding Fmoc-L-Aaa-RAM-Tentagel S resins were used applying the Fastmoc 0.1 mmol protocol. The assembly of the peptide sequence was achieved in iterative cycles in which the appropriate amino acids were coupled. In each cycle the N-Fmoc protecting group was removed by treating the resin with 20% piperidine in NMP (3 × 2.5 min). Amino acid couplings were performed using the N-Fmoc-protected amino acids (1 mmol, 10 eq. based on the resin) after preactivation with HBTU^{41,42} (1 mmol), HOBt⁴³ (1 mmol) and DIPEA (2 mmol) in DMF (20-30 min vortex). Remaining amino groups were acetylated with a mixture of Ac₂O (0.5 M), DIPEA (0.125 M), and HOBt (0.015 M) in NMP (10 min vortex). After the last coupling cycle the resins were treated with 20% piperidine in NMP (3 × 2.5 min) to remove the Fmoc group. Cleavages of the peptides were carried out by shaking the resins with a mixture of TFA, water and triisopropylsilane (18:1:1) for 3 h. The mixtures were filtered off, the resins were washed with TFA (3 × 3 mL) and the combined filtrates were co-distilled with toluene (3 × 25 mL). The residues were washed with cold Et₂O (4 × 5 mL), dissolved in 6 mL water and lyophilized.

Procedure for the syntheses of the biotinylated peptides. The peptides were synthesized following the general procedure. After the removal of the Fmoc-protective group the Fmoc-protected triethylglycol-spacer⁴⁴ (222 mg, 5 eq. based on resin) was coupled 2-times, using the Fastmoc 0.1 mmol protocol and the remaining free amino-groups were acetylated, with the capping-solution. The Fmoc-

protective group was removed afterwards and Biotin was coupled manually 2-times. Thereto Biotin (122 mg, 5 eq.) was preactivated in 2 mL NMP with HBTU (201 mg, 5.3 eq.), HOBt (72 mg, 0.53 mmol) and NMM (117 μL, 10.6 eq.) for 5 min. Afterwards the resin was vortexed with this solution for 1 h.⁴⁵ After the second coupling the remaining amino-groups were acetylated. The cleavage of the peptides from the resins was carried out as described above.

Biomimetic Calcium Carbonate Precipitation. The native peptides were used to test their vaterite-precipitating ability. For this purpose, we used the diffusion-based calcium carbonate precipitating method. Peptides were used in a concentration of 0.5 mg × mL⁻¹ as additive in this process. Briefly, 1 mL of a 10 mM calcium chloride solution was prepared with 0.5 mg × mL⁻¹ of peptide in a LoBind-Eppendorf tube, containing a freshly cleaned (acidic piranha) silicon dioxide glass-slide. The tube was sealed with parafilm and 3 to 5 small holes were pricked with a syringe. The tubes were introduced into a vacuum desiccator containing 7 g of freshly mortared ammonium carbonate. The resulting crystallization chamber was closed for 4 hours, leading to calcium carbonate precipitation by diffusion of ammonia and carbon dioxide into the calcium chloride solution. Subsequently, the silica glass slides were removed from the Eppendorf tube, carefully rinsed with MilliQ-water and dried at room temperature. The resulting precipitates were analyzed by SEM and micro-Raman spectroscopy and XRD.

Peptide binding specificity measurements. Freshly prepared vaterite nanoparticles were placed in a LoBind-EppendorfTM-tube and blocked with a BSA solution (1 mg mL⁻¹) in TBS to block unspecific binding sites. The resulting dispersion was mixed at 20°C for 1 h and centrifuged afterwards. The precipitate was washed six times with TBST (0.1% Tween 20) and 50 μL of a 50 μM peptide solution (biotinylated peptides Pep3 and Pep8) were added and the resulting dispersion was mixed at 20°C on a rotary shaker. After 1 h, the dispersion was centrifuged and washed six times with TBST. A 50 μL aliquot of an Alexa Fluor 488 conjugated streptavidine solution (0.1 μg mL⁻¹ in TBS) was added and the mixture incubated at 20°C for 30 minutes. The dispersion was centrifuged, washed six times with TBST and the precipitate was redispersed in ethanol. This dispersion was dropped onto a freshly cleaned glass slide and measured by fluorescence microscope. A second drop was put onto a TEM grid and measured with TEM.

Results and discussion

Phage Display and Uniqueness of Peptides. Our initial efforts involved a randomized heptamer peptide library (Ph.D.TM-7, New England Biolabs) with a theoretical diversity of 2 × 10⁹ displayed from the N-terminus of the pIII protein of the M13 bacteriophage (Fig. 1A). We used single crystalline vaterite nanoparticles⁴⁶ to enlarge the accessible surface and to decrease the variety of crystal surfaces. Vaterite nanoparticles with a BET surface area of approx. 50 m²g⁻¹ were prepared following ref. 38, and their crystallinity was confirmed by X-ray powder diffraction (PXRD). The as-prepared vaterite nanoparticles (Ø ≤ 50 nm, Fig. S1, Supporting Information) were used in the subsequent phage selection process. An aliquot of the original phage library was incubated with the target. After the washing steps the affinity of bound phages to vaterite nanoparticles was challenged under two different panning conditions. In the first and second panning round the particles were re-suspended in

0.2 mol L⁻¹/pH 2.2 glycine buffer, and the solution was neutralized subsequently with Tris (hydroxymethyl) aminomethane (Tris base, 1 mol L⁻¹, pH 9.1) according to the standard phage display protocol (Fig. 1B, left). In the third panning round, the phages were eluted by displacement using sodium acetate (Fig. 1B, right). The phage-bound particles were incubated in sodium acetate buffer (1 mol L⁻¹, pH 8.5, 30 min) and centrifuged afterwards to isolate acetate eluted phages. The particular advantage of this biopanning protocol and selection procedure with sodium acetate lies in its higher selectivity, which cannot be achieved with the standard protocol using HCl/glycine (pH 2.2). After each selection round, bacteria (*ER 2738 E. coli*) were infected with dilutions of the eluted phages and subsequently grown on IPTG/Xgal agar plates. Individual blue colony plaques (minimum 10 plaques) were selected and amplified in 1 mL of a 1:100 dilution of an overnight culture of *E. coli* for 4.5 h at 37°C. The amplified phages were separated as described above and the single-stranded phage-DNA was collected by standard phenol extraction. The DNA was re-suspended in 30 µL sterile distilled water and quantified by agarose gel electrophoresis and UV-Vis spectra at 260 nm. DNA sequencing was performed by StarSeq, and the sequences were translated into the corresponding peptides using the serial cloner software provided by SerialBasics.

A total of three selection rounds were performed as described above, with the isolation and sequencing of individual clones after each round (Fig. 2, all identified binders from the 3 rounds are given in Table S1, Supporting Information) Peptide sequences even from the first selection round against vaterite exhibit some evolutionary enrichment of amino acid functional groups, such as alcohol bearing side chains and positively charged basic residues (Fig. 2A and B) with only a small amount of acidic residues as assumed before.

The results from all selection rounds demonstrate a preferential placement of specific chemical functionalities within the peptide sequence, in particular the same positions of several clones (e.g. Pep3, Pep8), often adjacent to aliphatic residues. These trends were further exemplified in the results for round three. Following this selection round, a significant number of phage clones contained an alternating pattern of hydrophilic followed by hydrophobic side-chains. The sequence Pep8 lacks any acidic residue, but the basic arginine residue was found. In BLAST searches no restrictive domain of any known protein could be found. Still, the peptide was isolated from a highly selective elution mechanism, leading to the assumption of a highly vaterite-specific peptide sequence.

Overall the amino acid sequences include chemical moieties capable of electrostatic and hydrogen-bonding interactions, while the inclusion of proline provides the potential for structural features such as β -turns.^{47,48} The presence of alcohol-containing residues may be important for the synthesis of vaterite, which is accessible synthetically from alcohols, in particular ethylene glycol.^{38,49}

The peptides Pep3 and Pep8 were prepared by standard Fmoc solid phase peptide synthesis on a Rink-amide resins, yielding peptide amides as a phage-analogous system. In this way we avoided an influence of the carboxylic end on further measurements. Biotinylated peptides were synthesized for binding measurements using fluorescence microscopy. In addition we prepared a derivate of Pep8 (gPep8) in which a proline-residue is exchanged by glycine to probe the influence of this particular residue on the vaterite binding and precipitating ability.

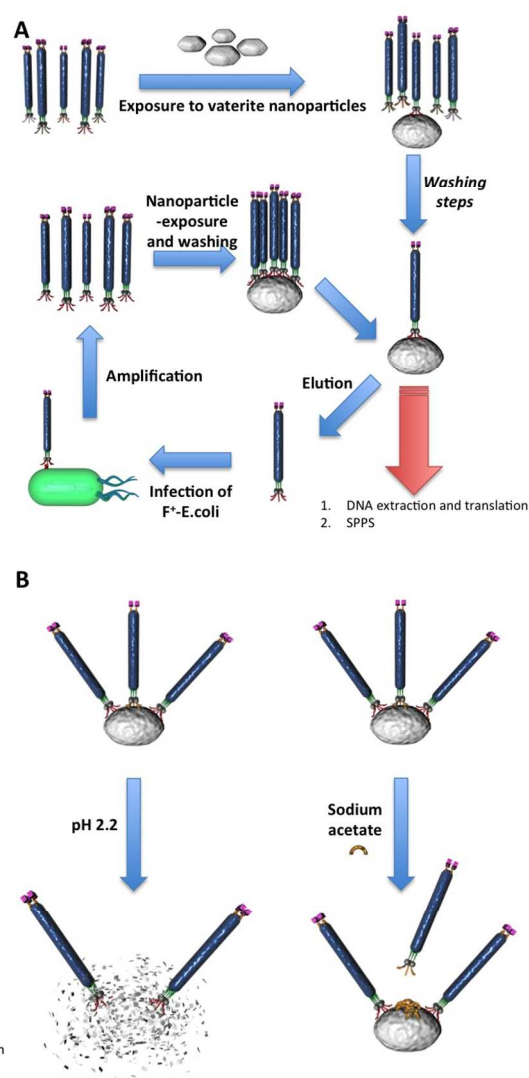


Fig. 1. A Phage display selection scheme for the identification of a phage with high affinity and specificity for vaterite nanoparticles. B Standard elution method (left) using pH 2.2 buffer and the displacement elution method (right) using sodium acetate.

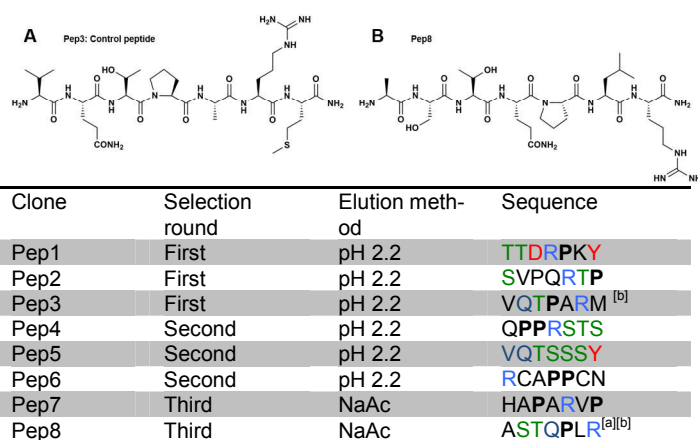


Fig. 2. Top: Control peptide VQTPARM (A, Pep3) and ASTQPLR (B, Pep8). Bottom: Selected sequences of peptides obtained from phage display selection against vaterite. Characteristic for nearly all peptides is the presence of proline (black).^[a] Sequence was found several times.^[b] Peptides synthesized by solid phase peptide synthesis (SPPS).

The binding specificities of the synthetic Pep3 (Fig. 2A) and Pep8 (Fig. 2B) peptides were investigated by fluorescence microscopy. The N-terminally biotinylated peptides were incubated with bovine serum albumine (BSA)-blocked vaterite. After incubation, the samples were washed and incubated with Alexa fluor 488-tagged streptavidin to image the location of the biotinylated peptides (Fig. 3). A second washing step was performed to eliminate non-specifically bound streptavidin. As a control, BSA-blocked particles were incubated only with dye-conjugated streptavidin. Imaging the peptide surface binding by confocal fluorescence microscopy (Fig. 3) revealed comparatively little adhesion of the Pep3 (1st panning) on vaterite (Fig. 3 (ii)), vs. control in (i) whereas peptide Pep8 (3rd panning) showed a very strong affinity (Fig. 3 (iii)). Thereby the difference in the binding affinity of Pep3 and Pep8 could be shown in a qualitative way. These findings provide evidence of a selection process with an increasing affinity by round of phage display. An analogous experiment was performed with a freshwater bivalve shell of *Diplodon chilensis patagonicus*.^{50,51} Usually the shells of *D. chilensis patagonicus* consist of a periostracum, a thin prismatic layer and a nacreous layer, but are only composed of aragonite.^{50,51} In contrast, the shell used in this experiment also contained vaterite.⁵¹ These vaterite surface structures could be distinguished from aragonite by using the biotinylated Pep8 (Fig. 3 (a and b)).

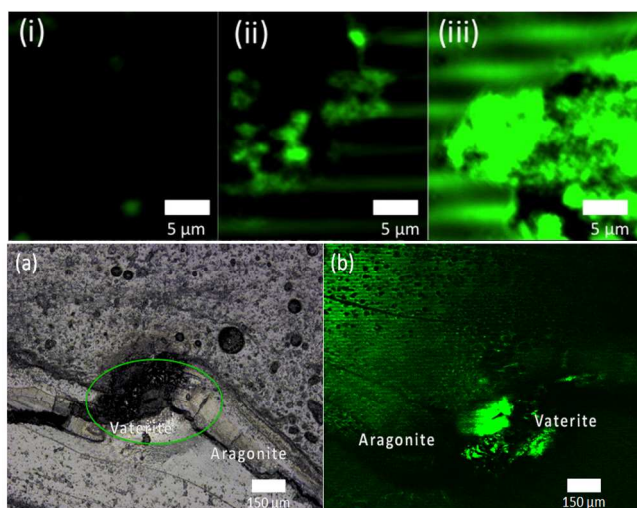


Fig. 3. Binding affinity measurements by biotin-streptavidin reaction. Fluorescence microscope images of biotinylated peptide-nanoparticle-adducts (i-iii) and freshwater mussel shell from *Diplodon chilensis patagonicus* (a,b) incubated with dye-conjugated streptavidin showing strong affinity between Pep8 and nanoparticles (iii) respectively biogenic vaterite (b).

Effect of "Point Mutations" on Binding. Point mutations, where the change of a single nucleotide causes a substitution of a different amino acid are quite common in nature, even in biomineralization. Point mutation can thus be silent/neutral or they can render the resulting protein non- or dysfunctional. To determine whether mutated, vaterite-specific peptides also had significant effects on the calcium carbonate growth we carried out CaCO₃ crystallization experiments. We synthesized a derivative of peptide Pep8 to probe the importance of particular residues for interfacial interactions and peptide vaterite binding. We focused on the proline motif which is assumed to play a critical role in binding because of its poor helix-forming propensities.^{47,48} Proline either breaks or kinks a helix, because of its inability

to form hydrogen bonds and also because its side chain interferes sterically with the backbone of the preceding turn.^{52,53} To determine the influences of proline in Pep8 we replaced the amino acid proline with glycine in the derivative gPep8 and carried out CaCO₃ crystallization and nanoparticle incubation experiments. Both peptides, the original Pep8 as well as its glycine-containing counterpart gPep8 were incubated with vaterite nanoparticles, and the outcome of the incubation was evaluated by scanning electron microscopy (SEM), transmission electron microscopy (TEM) and PXRD to check for vaterite-stabilizing or transformation effects. Crystallization experiments were carried out using the standard ammonium carbonate diffusion method in the presence of Pep8 and its glycine-containing counterpart gPep8. The basic peptide Pep8 only lead to the formation of vaterite as shown by SEM (Fig. 4A), PXRD and micro-Raman spectroscopy (Fig. S2 and 4, Supporting Information). Crystallization in the presence of the mutant peptide gPep8 lead exclusively to the formation of calcite as demonstrated again by SEM (Fig. 4B), PXRD (Fig. S3 and Table S2, Supporting Information) and micro-Raman spectroscopy, demonstrating the importance of proline in peptide Pep8. As evident from Fig. 4C the samples incubated with peptide Pep8 obtained from the 3rd panning contained phase-pure vaterite particles with an ellipsoidal habit as shown by PXRD and subsequent Rietveld refinement of the powder data (Fig. S3 and Table S3, Supporting Information). In comparison, the mutant variant gPep8 triggered a vaterite to calcite transformation (see Fig. 4D), verified again by PXRD (Fig. S3 and Table S3, Supporting Information).

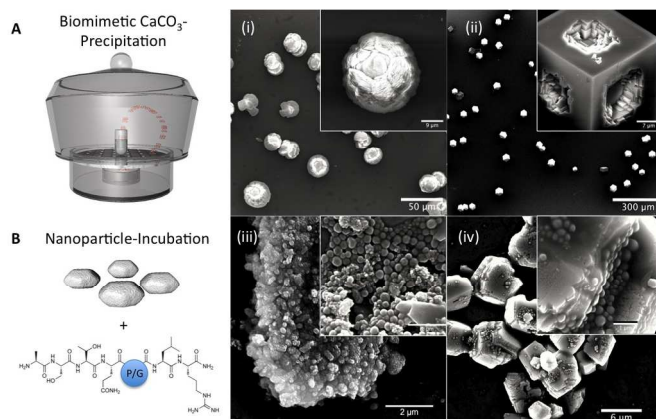


Fig. 4. Influence of Pep8 and its glycine-derivative gPep8 on calcium carbonate precipitation and nanoparticle incubation. A calcium carbonate precipitation in the presence of (i) Pep8 and (ii) gPep8 lead to the crystallization of vaterite (i) and calcite (ii). B Vaterite nanoparticle incubated in the presence of (iii) Pep8 and (iv) gPep8 rendered vaterite stable (iii) or triggered a phase transformation to calcite (iv).

Conclusions

Using phage display techniques combined with a displacement elution strategy we have identified a peptide sequence with highly specific binding to vaterite in the presence of aragonite, another crystalline polymorph of calcium carbonate. The peptide can recognize stereo-regularities and also small differences in the surface structure of vaterite and aragonite. In addition they even show the potential for a high degree of control over calcium carbonate polymorph crystalli-

zation. A significant number of peptides exhibited an alternating pattern of hydrophilic and hydrophobic side-chain functionalities. Importantly the peptides contain positively charged amino acids as well as proline rather than the expected negatively charged aspartate or glutamate units. This complements recent reports on the effect of positively charged polymers (and proteins) on calcite morphologies^{31,54-57} yielding thin films and fibers of CaCO₃ and of a novel basic protein acting as a key accelerator for crystal growth in nacre.³² In addition, A derivative of the identified peptide, in which proline was replaced by glycine showed a very different crystallization and transformation behavior. As subtle changes in the peptide structure generated large changes in the control over phase selection, this approach has great potential to offer new insights into how biopolymers precisely control mineral growth in natural systems. Molecular recognition (studied in this work) and matrix formation are two important processes associated with biomineralization. The highly specific peptides obtained in the studies reported here could be utilized as “anchor groups” with synthetic polymers (serving as matrix components) to form new peptide polymers to mimic biological mineralization processes^{13,14} or the self-aggregation of proteins involved in mineralization.^{58,59} Since large peptide-polymer libraries can be built from chemically diverse polymer blocks, we expect the discovery of highly effective hybrid peptide-polymers in the future.

Acknowledgements

This research was partially supported by the Deutsche Forschungsgemeinschaft (DFG) within the priority program 1569 “Generation of Multifunctional Inorganic Materials by Molecular Bionics”. The facilities of the Electron Microscopy Center in Mainz (EZMZ) were supported by the State Excellence Cluster COMATT and the SFB 625

Notes and references

- ^a Institut für Anorganische Chemie und Analytische Chemie, Johannes Gutenberg-Universität Mainz, Duesbergweg 10-14, D-55099 Mainz. Fax: +49 6131 39-25605; Tel: +49 6131 39-25135; E-mail: tremel@uni-mainz.de
- ^b Institut für Allgemeine Botanik, Johannes Gutenberg Universität, Müllerweg 6, D-55099 Mainz (Germany)
- ^c Institut für Geowissenschaften, Johannes Gutenberg-Universität Mainz, J.-J.-Becher-Weg 21, D-55099 Mainz (Germany). Present address: Department of Earth and Planetary Sciences, Macquarie University, NSW 2109, Australia.
- ^d Department Chemie, Ludwig-Maximilians-Universität München, Butenandtstr. 5-13, D-81377 München (Germany)
- Electronic Supplementary Information (ESI) available: Details of the measurement and refinement of the X-ray diffraction data for the crystallization of CaCO₃ with Pep8 and gPep8 (Table S1 and Fig. S1); details of the measurement and refinement of the X-ray diffraction data for the incubation of vaterite nanocrystals with Pep8 and gPep8 (Table S2 and Fig. S2); micro-Raman spectra for CaCO₃ crystallized in the presence of Pep8 and gPep8 (Fig. S3); Raman spectra of calcium carbonate precipitated in the presence of 1 mg·mL⁻¹ Pep8 (a) and gPep8 (b). Details of the peptide analysis. See DOI: 10.1039/b000000x/
- G. Falini, S. Albeck, S.; Weiner, L. Addadi, *Science* 1996, **271**, 67–69.
 - J. N. Cha, K. Shimizu, Y. Zhou, S. C. Christiansen, B. F. Chmelka, G. D. Stucky, D. E. Morse, *Proc. Natl. Acad. Sci. U.S.A.* 1999, **96**, 361–365.
 - N. Kröger, S. Lorenz, E. Brunner, M. Sumper, *Science* 2002, **298**, 584–586.
 - A. Sugawara, T. Nishimura, Y. Yamamoto, H. Inoue, H. Nagasawa, T. Kato, *Angew. Chem. Int. Ed.* 2006, **45**, 2876–2879.
 - S. R. Whaley, D. S. English, E. L. Hu, P. F. Barbara, A. M. Belcher, *Nature* 2000, **405**, 665–668.
 - R. R. Naik, S. J. Stringer, G. Agarwal, S. E. Jones, M. O. Stone, *Nat. Mater.* 2002, **1**, 169–172.
 - M. D. Roy, S. K. Stanley, E. J. Amis, M. L. Becker, *Adv. Mater.* 2008, **20**, 1830–1836.
 - S. V. Patwardhan, F. S. Emami, R. J. Berry, S. E. Jones, R. R. Naik, O. Deschaume, H. Heinz, C. C. Perry, *J. Am. Chem. Soc.* 2012, **134**, 6244–56.
 - H. A. Lowenstam, S. Weiner, *On Biomineralization*, Oxford University Press, New York, 1989.
 - F. Heinemann, M. Launspach, K. Gries, M. Fritz, *Biophys. Chem.* 2011, **153**, 126–153.
 - A. M. Belcher, X. H. Wu, R. J. Christensen, P. K. Hansma, G. D. Stucky, D. E. Morse, *Nature* 1996, **381**, 56–58.
 - M. Suzuki, K. Saruwatari, T. Kogure, Y. Yamamoto, T. Nishimura, T. Kato, H. Nagasawa, *Science* 2009, **325**, 56–58.
 - R. Lakshminarayanan, E. O. Chi-Jin, X. J. Loh, R. M. Kini, S. Valiyaveetil, *Biomacromolecules* 2005, **6**, 1429–1437.
 - P. A. Ajikumar, S. Vivekanandan, R. Lakshminarayanan, S. D. S. Jois, R. M. Kini, S. Valiyaveetil, *Angew. Chemie Int. Ed.* 2005, **44**, 5476–5479.
 - E. DiMasi, M. Olszta, V. Patel, L. Gower, *Cryst. Eng.* 2003, **5**, 346–350.
 - G. K. Hunter, J. O’Young, B. Grohe, M. Karttunen, H. A. Goldberg, *Langmuir* 2010, **26**, 18639–18646.
 - L. Addadi, S. Weiner, *Proc. Natl. Acad. Sci. U.S.A.* 1985, **82**, 4110–4114.
 - N. A. J. M. Sommerdijk, G. de With, *Chem. Rev.* 2008, **108**, 4499–4550.
 - N. A. Palchik, T. N. Moroz, *J. Cryst. Growth* 2005, **283**, 450–456.
 - F. K. Mayer, E. Weineck, *Jena. Z. Naturwiss.* 1932, **66**, 199–220.
 - L. Liao, Q.-L. Feng, Z. Li, *Crystal Growth & Design*, 2007, **7**, 275–279.
 - A. L. Soldati, D. E. Jacob, U. Wehrmeister, W. Hofmeister, *Mineral. Mag.* 2008, **72**, 577–590.
 - H. A. Lowenstam, D. P. Abbott, *Science* 1975, **188**, 363–365.
 - B. Hasse, H. Ehrenberg, J. C. Marxen, W. Becker, M. Epple, *Chem. Eur. J.* 2000, **6**, 3679–3685.
 - D. Ren, M. A. Meyers, B. Zhou, Q. Feng, *Mater. Sci. Eng. C* 2013, **33**, 1876–1881.
 - L. Kabalah-Amitai, B. Mayzel, Y. Kauffmann, A. N. Fitch, L. Bloch, P. U. P. A. Gilbert, B. Pokroy, *Science* 2013, **340**, 454–457.
 - R. Lakshminarayanan, X. J. Loh, S. Gayathri, S. Sindhu, Y. Banerjee, R. M. Kini, S. Valiyaveetil, *Biomacromolecules* 2006, **7**, 3202–3209.
 - S. Brown, *Proc. Natl. Acad. Sci. USA* 1992, **89**, 8651–8655.
 - M. Sarikaya, C. Tamerler, A. K.-Y. Jen, K. Schulten, F. Baneyx, *Nat. Mater.* 2003, **2**, 577–585.
 - A. B. Sanghvi, K. P. H. Miller, A. M. Belcher, C. E. Schmidt, *Nat. Mater.* 2005, **4**, 496–502.
 - B. Cantaert, Y. Y. Kim, H. Ludwig, F. Nudelman, N. A. J. M. Sommerdijk, F. C. Meldrum *Adv. Func. Mater.* 2012, **22**, 907–915.
 - D. Fang, C. Pan, H. Lin, Y. Lin, G. Zhang, H. Wang, M. He, L. Xie, R. Zhang, *J. Biol. Chem.* 2012, **287**, 15776–15785.
 - M. Suzuki, K. Saruwatari, T. Kogure, Y. Yamamoto, T. Nishimura, T. Kato, H. Nagasawa, *Science* 2009, **325**, 1388–1390.
 - F. C. Meldrum, H. Cölfen, *Chem. Rev.* 2008, **108**, 4332–4432.
 - C. Li, G. D. Botsaris, D. L. Kaplan, *Cryst. Growth Design* 2002, **2**, 387–393.
 - D. J. H. Gaskin, K. Starck, E. N. Vulfson, *Biotechnol. Lett.* 2000, **22**, 1211–1216.
 - D. Gebauer, A. Verch, H. G. Börner, H. Cölfen, *Crystal Growth Design* 2009, **9**, 2398–2303.
 - T. Schüler, W. Tremel, *Chem. Commun.* 2011, **47**, 5208–5210.
 - E. Bayer, W. Rapp, in *Chemistry of Peptides and Proteins*, (W. Voelter, E. Bayer, Y. A. Ovchinnikov, V.T. Ivanov, Eds.) *W. de Gruyter & Co., Berlin. New York*, (1986), 3.
 - H. Rink, *Tetrahedron Lett.* 1987, **28**, 3787–3790.
 - R. Knorr, A. Trzeciak, W. Baumwarth, D. Gillesen, *Tetrahedron Lett.* 1989, **30**, 1927–1930.

42. V. Dourtoglou, J.-C. Ziegler, B. Gross, *Tetrahedron Lett.* 1978, **19**, 1269-1272.
43. W. König, R. Geiger, *Chem. Ber.* 1970, **103**, 788-798.
44. S. Dziadek, *Entwicklung synthetischer Antitumorvakzine basierend auf komplexen tumorassoziierten Glycopeptidkonjugaten aus dem epithelialen Mucin MUC1*, PhD Dissertation: Mainz, 2005.
45. S. Keil, C. Claus, W. Dippold, H. Kunz, *Angew. Chem. Int. Ed.* 2001, **40**, 366-369.
46. E. Mugnaioli, I. Andrusenko, T. Schüler, N. Loges, M. Panthöfer, W. Tremel, U. Kolb, *Angew. Chem. Int. Ed.* 2012, **51**, 7041-7045.
47. E. G. Hutchinson, J. M. Thornton, *Protein Sci.* 1994, **3**, 2207-2216.
48. C. M. Wilmot, J. M. Thornton, *J. Mol. Biol.* 1988, **203**, 221-232.
49. M. Balz, H. A. Therese, J. Li, J. S. Gutmann, M. Kappl, L. Nasdala, W. Hofmeister, H.-J. Butt, W. Tremel, *Adv. Funct. Mater.* 2005, **15**, 683-688.
50. A. L. Soldati, D. E. Jacob, B. R. Schöne, M. M. Bianchi, A. Hadjuk, *J. Molluscan. Stud.* 2009, **75**, 75-85.
51. U. Wehrmeister, D. E. Jacob, A. L. Soldati, N. Loges, T. Häger, W. Hofmeister, *J. Raman Spectrosc.* 2011, **42**, 926 – 935
52. T. H. Creighton, *Proteins: structures and molecular properties*. W. H. Freeman, San Francisco, 1993.
53. C. N. Pace, J. M. Scholtz, *Biophys. J.* 1998, **75**, 422-427.
54. C. L. Freeman, J. H. Harding, D. Quigley, P. M. Rodger, *J. Phys. Chem. C* 2011, **115**, 8175-8183.
55. A.-W. Xu, M. Antonietti, H. Cölfen, Y.-P. Fang, *Adv. Funct. Mater.* 2006, **16**, 903-908.
56. Q. Yu, H.-D. Ou, R.-Q. Song, A.-W. Xu, *J. Cryst. Growth*, 2006, **286**, 178-183.
57. D. L. Masica, S.B. Schrier, E. Specht, J.J. Gray, *J. Am. Chem. Soc.* 2010, **132**, 12252-12262.
58. V. Pipich, M. Balz, S. Wolf, W. Tremel, D. Schwahn, *J. Am. Chem. Soc.* 2008, **130**, 6879-6892.
59. F. Natalio, T. Coralles, M. Panthöfer, I. Lieberwirth, D. Schollmeyer, W. E. G. Müller, M. Kappl, H.-J. Butt, W. Tremel, *Science* 2013, **339**, 1298-1302.